Laser Cooling from the Semi-Classical to the Quantum Regime.

J. DALIBARD and Y. CASTIN

Laboratoire de Spectroscopie Hertzienne de l'ENS (*)
24 rue Lhomond, F-75231 Paris Cedex 05, France

1. – Introduction.

The control of atomic motion by laser light is a field which has expanded very rapidly over the last few years. One of the most spectacular achievements in this domain is the possibility of reaching extremely low atomic kinetic temperatures, in the microkelvin range, by irradiating an atomic vapour with multiple quasi-resonant laser beams [1]. The limits of laser cooling in these so-called *optical molasses* correspond to r.m.s. velocities $\bar{v}$ of the order of only a few photon recoil velocities [2, 3]:

$$\bar{v} \simeq \text{a few } \frac{\hbar k}{M} , \tag{1}$$

where $\hbar k$ is the momentum of a photon involved in the cooling process and M is the atomic mass. One can even pass beyond this *recoil limit* using some improved cooling schemes [4, 5].

The combination of these low temperatures with the possibility of trapping the atoms around a given point in space offers a new unique tool for atomic spectroscopy and quantum optics, and many fields of atomic physics can benefit from these new techniques: metrology using atomic fountains [6, 7], collision physics [8-11], nonlinear optics [12, 13], etc.

These ultra-low temperatures also allow one to reach situations where the quantum nature of the atomic motion plays an important role. The atomic de

(*) Unité de recherche de l'Ecole Normale Supérieure et de l'Université Paris 6, associée au CNRS.

Broglie wavelength

$$\Lambda_{\mathrm{dB}} = \frac{h}{Mv} \tag{2}$$

is indeed quite large, of the order of a fraction of optical wavelength. This may be of great help for atomic interferometry experiments [14]. For sufficiently high atomic densities, this might also offer a way of observing collective quantum effects in a sample of cold neutral atoms.

This course is devoted to a description of various approaches to laser cooling of neutral atoms. We restrict here to the case of a closed atomic transition between a stable ground state g and an excited state e with a lifetime Γ^{-1} (see fig. 1). These two energy levels are separated by an energy $\hbar\omega_{\mathrm{A}}$ and they may both have a Zeeman degeneracy. The cooling laser field is supposed to be monochromatic, with an angular frequency ω_{L}.

The laser-cooling problem constitutes a model case for dissipation in quantum mechanics (see fig. 2): The *atom + laser field* system evolves coherently due to absorption and stimulated-emission processes, and it is dissipatively coupled to a *reservoir* formed by the quantized field in its ground state. This dissipative coupling corresponds to spontaneous-emission processes, and plays an essential role for interaction times longer than the excited lifetime Γ^{-1}.

We start in sect. 2 with a brief survey of the semi-classical description of

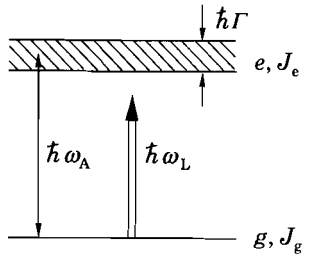

Fig. 1. – Closed atomic transition with a stable ground state g (angular momentum J_g) and an excited state e (angular momentum J_e) with a lifetime Γ^{-1}.

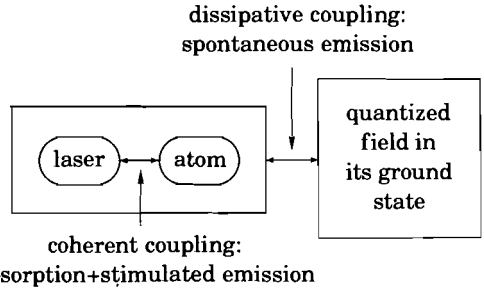

Fig. 2. – The interacting systems in a laser-cooling problem.

laser cooling, in which the atomic centre of mass is treated as a classical, pointlike particle. We present two cooling mechanisms, the Doppler-cooling scheme and the Sisyphus-cooling scheme. We then show that the limit of this second cooling mechanism requires a quantum treatment, which is presented in sect. 3. Finally sect. 4 is devoted to the description of a new, general approach to dissipative processes in quantum optics based on Monte Carlo wave functions and to a discussion of its application to laser-cooling problems.

2. – Semi-classical description of laser cooling.

2·1. *Validity of the semi-classical treatment.* – In order to treat the atom as a moving classical pointlike particle, two assumptions are necessary. The first condition ensures that the atomic position is well defined on the shortest spatial scale of variation of the laser field parameters (phase, polarization or intensity), *i.e.* the optical wavelength λ. This can be written

$$\Delta x \ll \lambda , \tag{3}$$

where Δx denotes the size of the atomic wave packet or, more precisely, the coherence length of the atomic-density operator (*e.g.*, the thermal de Broglie wavelength for a Boltzmann distribution).

The second condition ensures that the atomic velocity is well defined with respect to the velocity width of the atomic resonance. More precisely we require an uncertainty $k\Delta v$ on the Doppler shift much smaller than the width Γ of the atomic resonance:

$$k\Delta v \ll \Gamma . \tag{4}$$

Condition (4) can also be seen as the requirement that the spatial spreading of the atomic wave packet between two successive spontaneous emissions remains small as compared to λ. We assume here that spontaneous-emission processes occur with a rate Γ (saturated transition) and we use the fact that each of these processes decreases the coherence length of the atomic-density matrix to less than λ [15].

Clearly the two assumptions (3) and (4) are compatible with the Heisenberg inequality

$$M\Delta x \Delta v \geq \frac{\hbar}{2} \tag{5}$$

only if the following relation holds:

$$E_R = \frac{\hbar^2 k^2}{2M} \ll \hbar\Gamma . \tag{6}$$

This is the so-called *broad-line condition* which requires the recoil energy E_R to be much smaller than the energy width $\hbar\Gamma$ of the excited atomic level. We have indicated in table I the value of the ratio $\hbar\Gamma/E_R$ for the resonance line of three

TABLE I. – *Value of the «broad-line parameter» $\hbar\Gamma/E_R$ for various atoms used in laser-cooling experiments.*

Atom	$\hbar\Gamma/E_R$
H*	40
Na	400
Cs	2600

«typical» atoms, the metastable helium atom in the 2^3S_1 state, and the sodium and cesium atoms. We see that the broad-line condition is well satisfied for Na and Cs, but is only marginal for He*.

2·2. *The average radiative forces.* – Once the two conditions (3) and (4) hold, one can derive an expression for the average radiative force $\boldsymbol{f}$ acting on an atom located in a given position $\boldsymbol{r}$ and with a given velocity $\boldsymbol{v}$. Using Ehrenfest theorem, one gets [16, 17]

$$\boldsymbol{f} = \sum_{i=x,y,z} d_i \boldsymbol{\nabla} E_i(\boldsymbol{r}). \tag{7}$$

The force is proportional to the average atomic dipole $\boldsymbol{d}$ and to the gradient of the laser electric field $\boldsymbol{E}$ at the atom location. We now discuss these two contributions.

1) The laser electric field is assumed here to be monochromatic, and can, therefore, be written as

$$\boldsymbol{E}(\boldsymbol{r}) = \mathcal{E}(\boldsymbol{r})\,\boldsymbol{\varepsilon}(\boldsymbol{r}) \exp[-i(\omega t - \phi(\boldsymbol{r}))] + \text{c.c.} \tag{8}$$

The force related to the gradient of the phase $\phi(\boldsymbol{r})$ is called the radiation pressure force or scattering force, the force related to the gradient of the real amplitude $\mathcal{E}(\boldsymbol{r})$ is the dipole or gradient force, and finally the force related to the gradient of the complex unit vector $\boldsymbol{\varepsilon}(\boldsymbol{r})$ is simply named polarization gradient force.

2) The mean atomic dipole $\boldsymbol{d}$ is obtained from the average value of the atomic-dipole operator:

$$\boldsymbol{d} = \langle \boldsymbol{D} \rangle = \mathrm{Tr}(\rho_{\mathrm{at}} \boldsymbol{D}). \tag{9}$$

For a two-level atom without Zeeman degeneracy (*), the dipole operator $\boldsymbol{D}$ is

(*) This situation can be achieved in practice using a σ_+ polarized laser beam acting on a $J_g \leftrightarrow J_e = J_g + 1$ transition, in which case the atom is optically pumped on the transition $|g\rangle = |g, m_g = J_g\rangle \leftrightarrow |e\rangle = |e, m_e = J_e\rangle$. Note that there is no polarization gradient force in this case.

given by

$$\boldsymbol{D} = \boldsymbol{d}_0(|e\rangle\langle g| + |g\rangle\langle e|), \tag{10}$$

where $\boldsymbol{d}_0$ is the reduced dipole moment of the transition. For a more complex atomic transition in which the angular momenta of the ground and excited levels are taken into account, this atomic-dipole operator involves Clebsch-Gordan coefficients between ground and excited Zeeman sublevels [18]. The average value in (9) is taken over the steady-state atomic-density operator, calculated from the optical Bloch equations. This steady-state density operator can be calculated either for an atom at rest in $\boldsymbol{r}$ or for an atom dragged with a velocity $\boldsymbol{v}$ and passing in $\boldsymbol{r}$ at a given time.

We give here the expression of the radiative forces acting on a two-level atom at rest without Zeeman degeneracy. The radiation pressure force $\boldsymbol{f}_{\mathrm{RP}}$ and the dipole force $\boldsymbol{f}_{\mathrm{dip}}$ are given by [17]

$$\boldsymbol{f}_{\mathrm{RP}} = \frac{\hbar\Gamma}{2}\,\frac{s}{1+s}\,\boldsymbol{\nabla}\phi\,, \tag{11}$$

$$\boldsymbol{f}_{\mathrm{dip}} = -\,\frac{\hbar\delta}{2}\,\frac{\boldsymbol{\nabla}s}{1+s}\,, \tag{12}$$

where we have introduced the detuning $\delta = \omega_{\mathrm{L}} - \omega_{\mathrm{A}}$ between the laser and atom frequencies, the Rabi frequency $\Omega = 2\mathcal{C}\boldsymbol{d}_0\,\boldsymbol{\varepsilon}/\hbar$, and the saturation parameter

$$s = \frac{\Omega^2/2}{\delta^2 + \Gamma^2/4}\,. \tag{13}$$

2·3. *Fokker-Planck equation for the atomic phase space distribution.* – For slowly moving atoms, we obtain from (7) the force at first order in velocity

$$\boldsymbol{f}(\boldsymbol{r}, \boldsymbol{v}) = \boldsymbol{f}(\boldsymbol{r}, 0) - [\alpha(\boldsymbol{r})]\cdot\boldsymbol{v}\,, \tag{14}$$

where $[\alpha(\boldsymbol{r})]$ is the friction tensor, describing the damping of atomic motion in the optical molasses. In order to study the limit of cooling in these molasses, we need also to take into account the counterpart of cooling, which is the heating due to the randomness of spontaneous-emission processes.

In the semi-classical approach, this can be done by writing a Fokker-Planck equation for the evolution of the atomic centre-of-mass phase space distribution. Such an equation can be obtained in the limit

$$T_{\mathrm{int}} \ll T_{\mathrm{ext}}\,, \tag{15}$$

which corresponds to a situation where the internal atomic variables have a time response T_{int} much smaller than the time of evolution of external variables T_{ext}. It is valid for slow atoms ($k|v|T_{\mathrm{int}} \ll 1$) and it is obtained by eliminating the

internal dynamics adiabatically to get an equation for the external atomic phase space distribution, or, more precisely, the atomic-density matrix in the Wigner representation $w(\boldsymbol{r}, \boldsymbol{p}, t)$ [19,20]:

$$\frac{\partial w}{\partial t} = -\boldsymbol{v} \cdot \boldsymbol{\nabla}_r w - \sum_{i=x,y,z} \frac{\partial}{\partial p_i} ((f_i(\boldsymbol{r}, 0) - \alpha_{ij}(\boldsymbol{r}) v_j) w) + \\ + \sum_{i=x,y,z} D_{ij}(\boldsymbol{r}) \frac{\partial^2 w}{\partial p_i \partial p_j} . \tag{16}$$

This equation contains a free-flight term, a force term (see (14)), and finally a diffusion term describing the heating due to the randomness of spontaneous-emission processes. $D_{ij}(\boldsymbol{r})$ is the tensorial momentum diffusion coefficient.

The steady state of (16) gives the position and momentum equilibrium distributions for the atom and allows one in particular to derive a temperature for laser-cooled atoms. A simple approximate solution of this equation is obtained by assuming a spatially uniform distribution w. Due to the spatial periodicity of optical molasses, $\boldsymbol{f}(\boldsymbol{r}, 0)$ averages to 0, and one is left in the isotropic case with the simpler equation

$$\frac{\partial w}{\partial t} = \boldsymbol{\nabla}_p (\bar{\alpha} \boldsymbol{v} w) + \bar{D} \boldsymbol{\nabla}_p^2 w , \tag{17}$$

whose solution is Gaussian, with an effective temperature which can be written in terms of the spatially averaged friction and diffusion coefficients:

$$k_B T = \frac{\bar{D}}{\bar{\alpha}} . \tag{18}$$

Let us briefly conclude with some comments on the validity of (18). First, we have to check in each particular situation that this kinetic energy $k_B T$ is larger than the depth of the wells which may be created by $\boldsymbol{f}(\boldsymbol{r}, 0)$. If it is not the case, the assumption of a spatially uniform steady-state distribution is clearly not valid. Second, we have to give some estimate for the validity condition (15) of the general Fokker-Planck equation (16). A typical internal time is $T_{\text{int}} \sim \Gamma^{-1}$ for a two-level atom without Zeeman degeneracy, while external time will be found in the following to be of the order of $M/\hbar k^2$ or longer. The broad-line condition then ensures that (15) is verified. For an atom with Zeeman degeneracy in the ground state, this is not true any more because there may appear very long pumping times which reverse the inequality of (15) and make this Fokker-Planck approach unapplicable.

2·4. *Doppler cooling.* – We consider here the one-dimensional situation represented in fig. 3. An atom is moving in the field created by two counterpropagating plane running waves, detuned red from resonance ($\omega_L < \omega_A$) [21,22]. We assume that the two running waves are weak and do not saturate the atomic transition. Then we can obtain the total force acting on the atom by adding in-

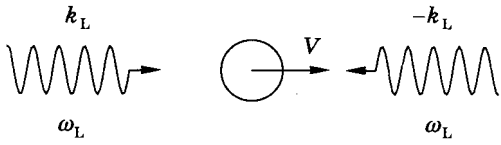

Fig. 3. – Doppler cooling in 1D optical molasses.

dependently the radiation pressure forces created by each running wave [23]. Due to the choice $\omega_L < \omega_A$ and because of Doppler effect, a moving atom sees the counterpropagating wave closer to resonance than the copropagating one. Consequently, for an atom moving, for instance, to the right as in fig. 3, the radiation pressure force created by the counterpropagating wave coming from the right is larger than the radiation pressure force exerted by the copropagating wave coming from the left. Therefore, a moving atom feels a net force opposed to its velocity. This friction force damps the atomic motion and the atom is cooled.

Using the expression (11) for the radiation pressure force created by each travelling wave and replacing δ by $\delta \pm kv$ to take into account Doppler effect, we obtain for the net force acting on a moving atom in the limit $k|v| \ll |\delta|$

$$f = -\bar{\alpha} v , \tag{19}$$

where the friction coefficient $\bar{\alpha}$ is given by

$$\bar{\alpha} = \hbar k^2 s_0 \frac{2|\delta|\Gamma}{\delta^2 + \Gamma^2/4} . \tag{20}$$

We note, as announced above, that the external time $M/\bar{\alpha}$ associated with this damping is larger than $M/\hbar k^2$, since $s_0 \ll 1$.

The momentum diffusion coefficient can be estimated simply by noting that, due to the randomness of the number of absorbed photons per unit time and the randomness of the momentum carried away by the spontaneously emitted photon, the atomic momentum performs a random walk with a step $\hbar k$ and a rate $\sim 2\Gamma s_0$. This gives

$$\bar{D} = \hbar^2 k^2 \Gamma s_0 . \tag{21}$$

Using (18), we now get the temperature of Doppler-cooled atoms. The temperature is minimal for a detuning $\delta = \omega_L - \omega_A$ equal to $-\Gamma/2$, and it is given by [24]

$$k_B T = \frac{\hbar\Gamma}{2} . \tag{22}$$

This gives temperatures in the range of 100 μK. More precisely, for the 3 atoms considered above, one obtains 36 μK for He*, 240 μK for Na and 120 μK for Cs. We note that, for atoms cooled at the Doppler limit (22), the r.m.s. vel-

ocity $\bar{v}$ and the de Broglie wavelength (*i.e.* coherence length Δx) are given by

$$\bar{v} = \sqrt{\frac{\hbar\Gamma}{2M}}\,, \tag{23}$$

$$\Lambda_{\mathrm{dB}} = \Delta x = 2\pi\sqrt{\frac{2\hbar}{M\Gamma}}\,, \tag{24}$$

so that both conditions (3) and (4) are simultaneously fulfilled in the broad-line limit:

$$\frac{\Delta x}{\lambda} = \sqrt{\frac{2\hbar k^2}{M\Gamma}} \ll 1\,, \tag{25}$$

$$\frac{k\bar{v}}{\Gamma} = \sqrt{\frac{\hbar k^2}{2M\Gamma}} \ll 1\,. \tag{26}$$

This shows that, in the broad-line limit, it is legitimate to use a semi-classical treatment to derive the Doppler-cooling limit.

2·5. *Sisyphus cooling.* – Sisyphus cooling is the simplest example of laser cooling with polarization gradients. It uses the Zeeman structure of the ground atomic state to provide a cooling which is much more efficient than Doppler cooling. The search for cooling mechanisms other than Doppler has been initiated by the discovery of anomalously low temperature in optical molasses, well below the Doppler-cooling limit [2], and the role of polarization gradients has been emphasized shortly after [25, 26].

In one dimension, two types of polarization gradient, corresponding to two different cooling mechanisms, have been identified [27-29]. The first one is obtained with two plane waves with orthogonal linear polarizations (fig. 4*a*)). The axes of the resulting polarization are constant, oriented at 45° with respect to

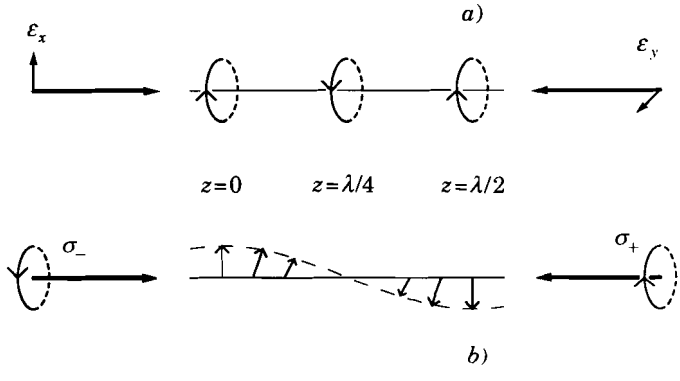

Fig. 4. – The two limiting cases of polarization gradient in one dimension. *a*) The lin ⊥ lin configuration, with a gradient of ellipticity and constant axis of polarization. *b*) The σ_+-σ_- configuration, with a resulting rotating linear polarization.

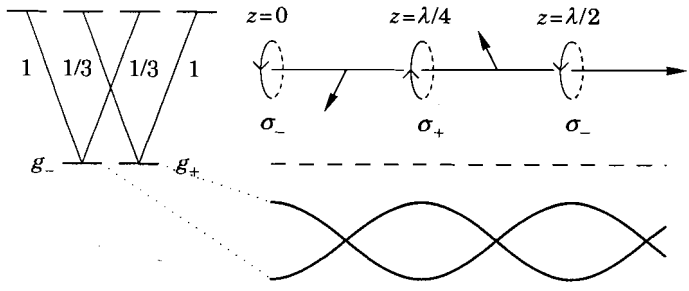

Fig. 5. – Light-shifted ground-state energy levels of a $J_g = 1/2 \leftrightarrow J_e = 3/2$ atom in a lin $\perp$ lin laser field. Due to the gradient of ellipticity of the light, the two Zeeman sublevels oscillate in phase opposition with a period $\lambda/2$.

the polarization axis of the incoming beams. The ellipticity of the resulting polarization varies in space, going from circular to linear over a distance of $\lambda/8$. This configuration leads to Sisyphus cooling, as we show below. The second configuration is obtained with two incoming waves with orthogonal circular polarizations (fig. 4*b*)). The resulting polarization in this σ_+-σ_- configuration is linear everywhere (no gradient of ellipticity), and its direction rotates with a period $\lambda/2$. This configuration leads to orientational cooling.

We now focus on the situation of fig. 4*a*) and we consider the motion of an atom with an angular momentum $J_g = 1/2$ in the ground state and $J_e = 3/2$ in the excited state (see fig. 5)(*). We restrict ourselves to the low-saturation domain:

$$s_0 = \frac{\Omega^2/2}{\delta^2 + \Gamma^2/4} \ll 1 , \tag{27}$$

which is known experimentally to lead to the lowest temperatures. In (27), $\Omega = 2 d_0 \mathcal{E}_0/\hbar$, where d_0 is the reduced dipole moment of the transition, and $\mathcal{E}_0$ the field amplitude in each travelling wave. When (27) is fulfilled, the atoms remain mostly in their internal ground-state sublevels. In the following, we also restrict to situations where the Doppler shifts can be neglected compared to Γ. Therefore, we ignore here the Doppler-cooling mechanism presented in subsect. 2·4. We decompose the effect of the laser light on the atoms into two parts. We first consider the reactive part, *i.e.* the shifts of the levels caused by the light. We then study the dissipative part of this coupling, corresponding to the real transitions between the ground-state sublevels associated with spontaneous-emission processes.

We consider as for Doppler cooling a negative detuning, so that the two Zee-

(*) The simpler atomic transition $J_g = 0 \leftrightarrow J_e = 1$ would not lead to any additional cooling with respect to Doppler cooling.

man substates are shifted downwards. The key point is that the size of the shift of each substate depends on the location of the atom. If the atom is located at a place where the light is σ_- polarized ($z = 0$ in fig. 5), the shift of level $|g_-\rangle = |g, m = -1/2\rangle$ is three times bigger than the shift of level $|g_+\rangle = |g, m = 1/2\rangle$, because of the intensity factors (squares of Clebsch-Gordan coefficients) of the $m_e - m_g = -1$ transitions, as indicated in fig. 5. At a place where the light is σ_+ polarized ($z = \lambda/4$ in fig. 5), the conclusion is reversed and the level $|g_+\rangle$ is shifted three times more than the level $|g_-\rangle$. In a place where the light is linear, one finds by symmetry that the two shifts are equal. Going through a small algebra, we obtain that the reactive part of the atom-laser coupling consists in a periodic potential $U_\pm(z)$, depending on the atomic ground-state sublevel $g_\pm$:

$$U_\pm(z) = \frac{U_0}{2}(-2 \pm \cos 2kz) \qquad \text{with } U_0 = -\frac{2}{3}\hbar\delta s_0 . \tag{28}$$

We now consider the transitions between g_+ and g_- caused by spontaneous emissions; these optical-pumping processes also depend on the location of the atom. Suppose that the atom is moving towards the right and starts in $z = 0$ in level g_- (fig. 6). At this place since the light is σ_-, the atom cycles on the transition $|g, m = -1/2\rangle \leftrightarrow |e, m = -3/2\rangle$ and can never jump to the level g_+. Therefore, it has to climb uphill until it reaches a place where there is a sufficient amount of σ_+ light so that the atom can be optically pumped to g_+ by a sequence $|g, m = -1/2\rangle \rightarrow |e, m = 1/2\rangle \rightarrow |g, m = 1/2\rangle$. This occurs preferentially around $z = \lambda/4$, at the top of $U_-(z)$, where the light is purely σ_+, and the atom is then put in a valley for $U_+(z)$. Once in level g_+ in z close to $\lambda/4$, the atom has little chance to come back to g_-, because the light is essentially σ_+ polarized

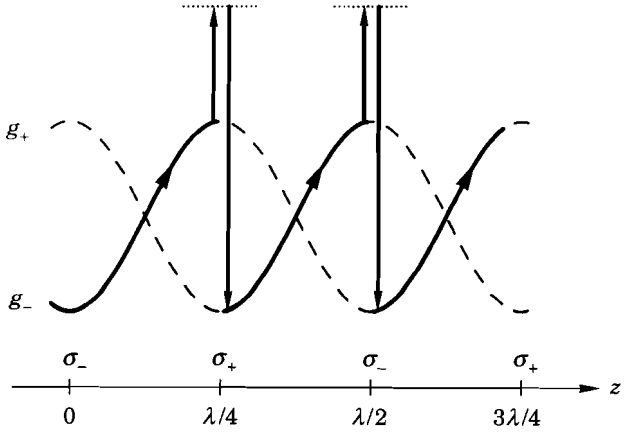

Fig. 6. – Sisyphus effect: due to the spatial variation of the optical-pumping rates, a moving atom climbs more than it goes down in its energy diagram. This causes a damping of its velocity in a much more efficient way than Doppler cooling.

at this place. The atom has, therefore, to climb again in $U_+(z)$ until it reaches a place where there is a noticeable fraction of σ_- light, which can pump it back to g_-.

It is clear that the atom loses energy in this process since it climbs more than it goes down. This is in close analogy with the Sisyphus myth in the Greek mythology where Sisyphus was sentenced by the Gods to push a rock forever to the top of a mountain, the rock rolling back to the valley each time it had reached the top. For this atomic Sisyphus process, it is instructive to make a balance of momentum and energy exchange. As the atom climbs uphill, it converts kinetic energy into potential energy, its total energy remaining constant. The decrease of momentum of the atom is due to a redistribution of photons between the two travelling waves forming the polarization gradient. Then, when the atom jumps from the top of a hill to a valley, it spontaneously emits a photon whose energy is higher than the laser photon energy by the height of the hill. This transition decreases the potential energy of the atom, while leaving its kinetic energy unchanged if one neglects the recoil associated with the spontaneous emission of the photon.

If we now take into account the recoil in spontaneous-emission processes, we have to add to the previous reasoning the corresponding heating, which puts a threshold for the potential depths U_0 [15,18]. Each fluorescence cycle, *i.e.* absorption of a laser photon spontaneous emission of a fluorescence photon, can be shown to lead to an increase of kinetic energy ($(41/30)E_R$). Among those cycles, only a fraction of 1/6 contributes to cooling, by changing the internal atomic state: $g_+ \to e \to g_-$ or $g_- \to e \to g_+$. The average loss of energy for these cooling cycles is $U_0/2$, so that we find that there is a net cooling effect only if

$$U_0 > (82/5)E_R \,. \tag{29}$$

The intuitive limit of Sisyphus cooling corresponds to a situation where the energy of the atom is of the order of or smaller than the potential modulation depth U_0. In this case, the atom does not have a sufficient kinetic energy to climb the potential hills, and it gets trapped in the potential valleys of $U_\pm(z)$. This intuitive reasoning is confirmed by a semi-classical treatment where one calculates a friction coefficient and a momentum diffusion coefficient, averaged over a wavelength [28]. The friction coefficient is found to be independent of the light intensity:

$$\bar{\alpha} = 3\hbar k^2 \frac{-\delta}{\Gamma} \tag{30}$$

and the equilibrium temperature is given by

$$k_B T = \frac{3}{8} U_0 \,. \tag{31}$$

This indicates that small temperatures should be obtained with small laser intensities and large detunings.

Let us discuss briefly the validity of this semi-classical result. First we note that the result (31) can only be qualitatively correct since we obtained it assuming a uniform spatial atomic distribution, and we predict at the same time a temperature of the order of the potential-well depth U_0 (subsect. 2·3). We now compare the optical-pumping relaxation time for internal variables, $T_{\text{int}} \simeq \simeq 1/\Gamma s_0$, with the characteristic time T_{ext} for external variables. We take here

$$T_{\text{ext}} \simeq M/\bar{\alpha} \text{ or } 1/\Omega_{\text{osc}} , \tag{32}$$

which corresponds to either the velocity damping time or the oscillation period in the bottom of the potential well (28). Both choices lead to the same expression for the validity condition (15):

$$T_{\text{int}} \ll T_{\text{ext}} \Leftrightarrow U_0 \gg \frac{\delta^2}{\Gamma^2} E_{\text{R}} . \tag{33}$$

One can check that this validity condition is also equivalent to the requirement $k\bar{v}\, T_{\text{int}} \ll 1$, where $\bar{v}$ is the r.m.s. velocity deduced from (31). This last condition ensures that it is legitimate to keep only the first-order velocity components in the expression of the force acting on the atom, for all the velocity classes populated in steady state (see (14)). For a given detuning, the validity condition (33) puts a lower bound on the intensity and, therefore, on the temperature that one can predict in this model:

$$k_{\text{B}} T \gg k_{\text{B}} T_{\min} \sim E_{\text{R}} \frac{\delta^2}{\Gamma^2} . \tag{34}$$

We finally note that, between the threshold (29) and the lower bound (33), there is for $|\delta| \gg \Gamma$ a large range of values of U_0 for which Sisyphus cooling is expected to work, but cannot be described by the previous semi-classical treatment. We show in the next section how to fill this gap using a quantum approach.

3. – The quantum regime of Sisyphus cooling.

3·1. *Experimental and numerical results.* – Let us now compare the predictions (31), (34) of the simple semi-classical model of Sisyphus cooling presented above with results obtained either experimentally or numerically. We have plotted in fig. 7 temperature measurements which have been obtained with Cs atoms [3]. These data show a very good qualitative agreement with (31). The temperature varies linearly with $U_0 \sim \Omega^2/|\delta|$ over a wide range of laser intensities and detunings, and the proportionality coefficient differs by less than a

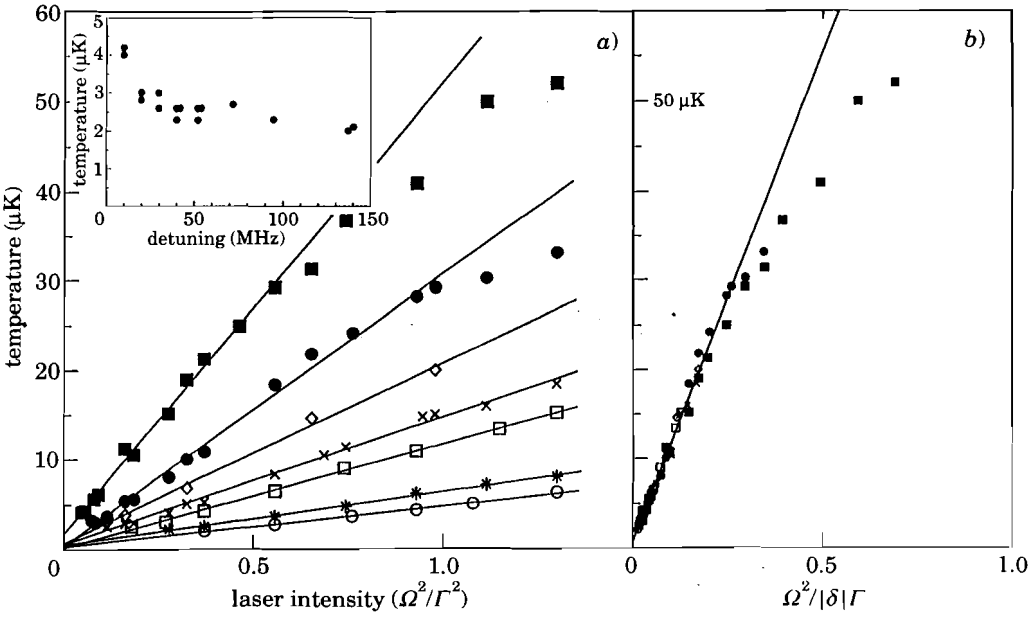

Fig. 7. – Temperature measurements of Cs atoms in optical molasses, as a function of laser intensity and detuning. *a*) Temperature *vs.* intensity at fixed detuning. Insert: lowest temperature achieved as a function of detuning. *b*) Temperatures of *a*) plotted against $\Omega^2/|\delta|$. The straight line is a fit to the points with small $\Omega^2/|\delta|$. The «universal law» $k_B T \sim \Omega^2/|\delta|$ is valid until $k_B T \sim 10 E_R$; $|\delta|/2\pi$: ■ 10 MHz, ● 20 MHz, ◇ 30 MHz, × 40 MHz, □ 54 MHz, * 95 MHz, ○ 140 MHz.

factor 3 from the one appearing in (31). This agreement is very remarkable if one notes that temperature measurements were done in 3D, while (31) is a 1D prediction. Also the Cs transition is $J_g = 4 \leftrightarrow J_e = 5$, quite far from our $J_g = 1/2 \leftrightarrow J_e = 3/2$ model.

However, an important difference appears between the semi-classical model and those experimental results, that we already noticed at the end of the previous section and which indicates the need for a more elaborate treatment. The lowest temperatures are obtained for detunings large compared to Γ. For such a detuning, as one decreases the laser intensity, the molasses works well until one reaches a temperature of the order of $10E_R$. This limit, which is in good qualitative agreement with (29), is independent of detuning and is well below the bound (34). This indicates that many points of fig. 7, and in particular the coldest ones, are not within the validity region of the semi-classical treatment given by (33).

This difference also appears in a complete numerical treatment of 1D Sisyphus cooling for a $J_g = 1/2 \leftrightarrow J_e = 3/2$ transition in which one looks for the steady state of the total (internal + external) atomic-density matrix [15, 30]. The steady-state r.m.s. velocity is plotted in fig. 8 in units of the recoil velocity,

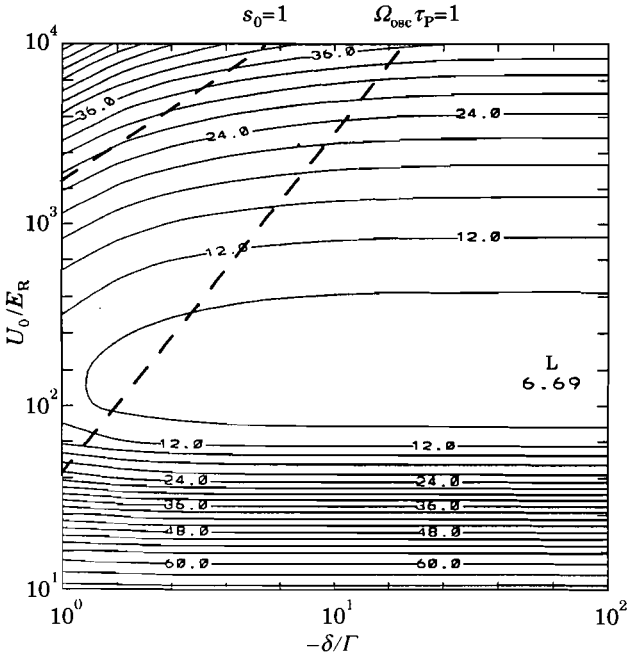

Fig. 8. – Contour plot of the r.m.s. velocity $\bar{v}$ in 1D Sisyphus cooling for the Cs atom parameters. The lowest velocities are of the order of 6.7 recoil velocities. They are obtained for a set of parameters δ, U_0 well outside the validity region of the semi-classical treatment. This validity region is below the high-saturation domain indicated by the line $s_0 = 1$, and above the dotted line $\Omega_{osc}\tau_P = 1$, where $\tau_P = 9/2\Gamma s_0$ is the optical-pumping time.

as a function of the detuning $|\delta|/\Gamma$ and the optical-well depth U_0/E_R. We have also shown in this figure the validity domain of the semi-classical approach (33). One clearly sees that the smallest r.m.s. velocities are obtained for a set of parameters outside the semi-classical validity region (*).

It is, therefore, necessary to elaborate another theoretical treatment for describing laser cooling in the regime $T_{int} > T_{ext}$. One could first think of an improved semi-classical treatment, by taking into account the velocity dependence of friction and diffusion, and also the spatial variation of the atomic distribution. However, it is actually easier to go directly to a quantum treatment of atomic motion, which will in addition lead to the predictions of new quantum effects related to the trapping of the atoms in the optical wells.

3·2. *Principle of a quantum treatment.* – We have seen both experimentally and numerically that the parameters δ and Ω, or equivalently δ and U_0, leading

(*) For numerical reasons, this plot has been calculated with a simplified dipole radiation pattern, which slightly overestimates the heating due to spontaneous photon recoil.

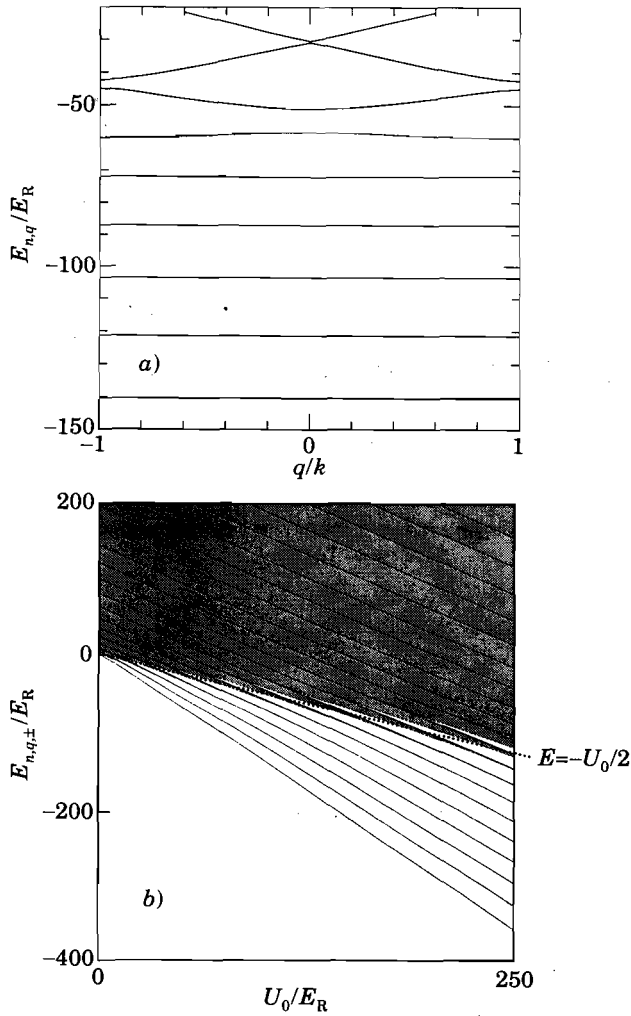

Fig. 9. – Band structure of the energy spectrum of H_ε for $U_0/E_R = 100$ (*a*)) and as a function of U_0/E_R (*b*)). The shaded areas correspond to allowed energies. For a given U_0, the energies above $-U_0/2$ corresponding to an above-barrier motion are mostly allowed (quasi-free motion). On the opposite, the energy bands corresponding to a bound classical motion ($-3U_0/2 < E < -U_0/2$) are very narrow, except in the immediate vicinity of $U_0/2$.

The eigenvalue problem

$$-\frac{\hbar^2}{2M}\frac{d^2\psi_{n,q}(z)}{dz^2} + U_+(z)\psi_{n,q}(z) = E_{n,q}\psi_{n,q}(z) \tag{41}$$

can be cast into a universal one using the reduced units $\zeta = kz$, U_0/E_R, E_{nq}/E_R:

$$(42) \qquad -\frac{d^2\psi_{n,q}(\zeta)}{d\zeta^2} + \frac{U_0}{2E_R}(-2+\cos 2\zeta)\psi_{n,q}(\zeta) = \frac{E_{n,q}}{E_R}\psi_{n,q}(\zeta).$$

The spectrum of H_ε is indicated in fig. 9*a*) for $U_0/E_R = 100$, which is close to the optimum situation appearing in fig. 8. We find 6 bands corresponding to bound states ($E_{n,q} < -U_0/2$); the width of the lowest band $n = 0$ is extremely small ($10^{-6}E_R$). A plot of the energy spectrum as a function of U_0/E_R is indicated in fig. 9*b*). It shows that the number of «bound bands» increases as $\sqrt{U_0/E_R}$, as does the splitting $\hbar\Omega_{osc}$ between two adjacent bands.

3·4. *Steady-state populations.* – We now take into account the transitions induced by optical-pumping processes between the various $|n, q, \varepsilon\rangle$. As we have emphasized above, the density matrix in the secular approximation can be described only in terms of the populations $\pi_{n,q,\varepsilon}$ of those eigenstates.

In steady state, we have

$$(43) \qquad 0 = \dot{\pi}_{n,q,\varepsilon} = -\pi_{n,q,\varepsilon}\sum_{n',q',\varepsilon'}\gamma(n, q, \varepsilon \to n', q', \varepsilon') + \sum_{n',q',\varepsilon'}\gamma(n', q', \varepsilon' \to n, q, \varepsilon)\pi_{n',q',\varepsilon'}.$$

The rates $\gamma(n, q, \varepsilon \to n', q', \varepsilon')$ are derived from the master equation describing optical-pumping processes. We will not perform a detailed calculation for

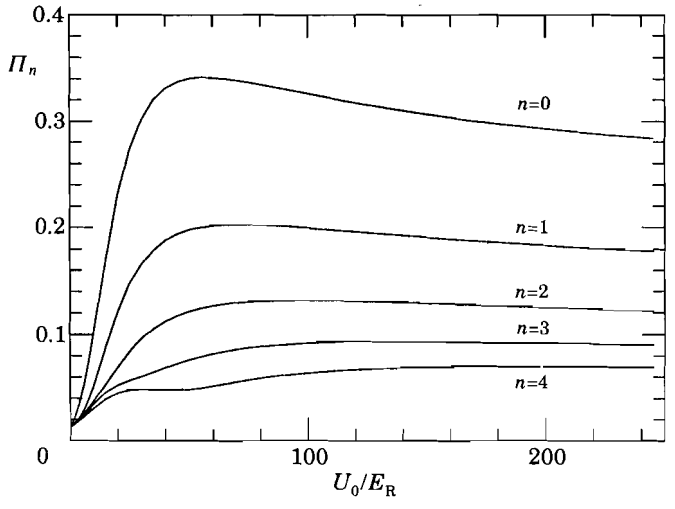

Fig. 10. – Steady-state populations of the various energy bands, as a function of U_0/E_R. This calculation has been done taking into account the first 80 bands, with 6 values for q in each band.

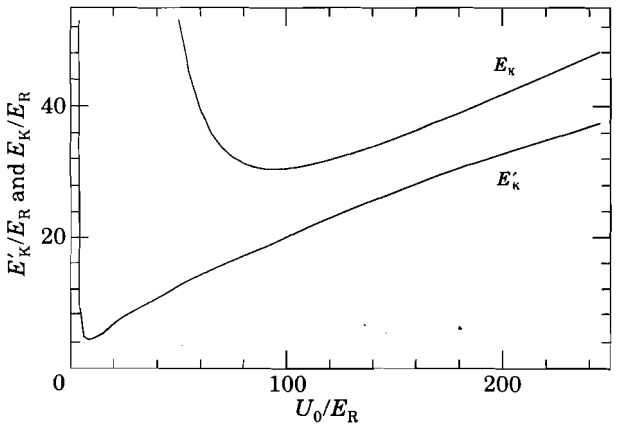

Fig. 12. – Steady-state kinetic energies $E_K = M\bar{v}^2/2$ and $E'_K = M\,\delta v^2/2$ (where δv is the half-width at $\exp[-1/2]$ of the velocity distribution) as a function of U_0. These two quantities would be equal for Gaussian velocity distributions.

the average kinetic energy $E_K = M\bar{v}^2/2$ as a function of U_0. It is minimal for $U_0/E_R = 95$, with $\bar{v} \simeq 5.5\,\hbar k/M$.

3·5. *Conclusions for this approach.* – The general features of this quantum treatment are in good qualitative agreement with experimental and numerical results of subsect. 3·1. The most striking result is the existence of a universal parameter U_0/E_R. This universality appears clearly in fig. 8 where the contour lines are parallel with the δ axis in the region $\Omega_{osc} T_{int} \ll 1$, indicating that here also the results depend only on U_0/E_R. Also both the variations of the steady-state atomic kinetic energy with U_0 and the order of magnitude of the minimum $\bar{v}$ are in agreement with the numerical results shown in fig. 8.

This approach also gives access to other observable quantities of laser-cooled atomic samples, more deeply connected to the quantization of atomic motion, such as the discrete structure of the energy spectrum. These quantum features have recently been observed in two spectroscopy experiments, one dealing with the absorption spectrum of the cold atomic sample [32], the other one with the fluorescence spectrum [33]. Also an experiment in Stony Brook has shown the existence of strong magnetic r.f. resonances in laser-cooled samples produced by M.I.L.C. (magnetically induced laser cooling), which may be related to transitions between the quantized levels [34].

This treatment can clearly be generalized to other transitions and other cooling schemes. We have extended it to the 1D Sisyphus cooling of a $J_g = 1 \leftrightarrow J_e = 2$ transition [15], and also to the study of Sisyphus cooling in 2D [35]. BERGEMAN has used a similar approach to study the M.I.L.C. situation [36]. Also COURTOIS and GRYNBERG have used such an approach to

give a quantitative analysis of the spectroscopy experiments showing the atomic quantization mentioned above [37].

4. – A Monte Carlo wave function approach.

We now turn to the last part of this lecture which is devoted to the description of a new general method which can be used for the theoretical study of dissipative processes in quantum optics and atomic physics, such as laser cooling. Usually the dissipative coupling between a small system and a large reservoir can be treated by a master-equation approach [38-41]; one writes a linear equation for the time evolution of the reduced-system density matrix $\rho_S = \mathrm{Tr}_{res}(\rho)$, trace over the reservoir variables of the total density matrix. If we denote H_S the Hamiltonian for the system, this equation can be written

$$\dot{\rho}_S = \frac{i}{\hbar}[\rho_S, H_S] + \mathscr{L}_{relax}(\rho_S). \tag{45}$$

In (45), $\mathscr{L}_{relax}$ is the relaxation superoperator, acting on the density operator ρ_S. It is assumed here to be local in time, which means that $\dot{\rho}_S(t)$ depends only on ρ_S at the same time (Markov approximation). All the system dynamics can be deduced from (45). One can calculate one-time average values of a system operator A: $a(t) = \langle A \rangle(t) = \mathrm{Tr}(\rho_S(t)A)$, and also, using the quantum regression theorem [42], multitime correlation functions such as $\langle A(t+\tau)B(t) \rangle$.

We present here an alternative treatment based on a Monte Carlo evolution of wave functions of the small system (MCWF) [43-46]. This evolution consists of two elements: evolution with a non-Hermitian Hamiltonian, and randomly decided «quantum jumps», followed by wave function normalization. This approach, which is equivalent to the master-equation treatment, has two main interests. First, new physical insight may be gained, in particular in the studies of the behaviour of a single quantum system. Second, if the relevant Hilbert space of the quantum system has a dimension N large compared to 1, the number of variables involved in a wave function treatment ($\sim N$) is much smaller than the one required for calculations with density matrices ($\sim N^2$). For the problem of laser cooling in the quantum regime which is of interest here, N stands for the number of internal + external atomic states, and is indeed $\gg 1$. The MCWF approach may, therefore, bring an important gain in computing time compared with the density matrix treatment used, for instance, for getting the results plotted in fig. 8.

4·1. *The* MCWF *procedure.* – The class of relaxation operators that we consider here is the following:

$$\mathscr{L}_{relax}(\rho_S) = -\frac{1}{2}\sum_m (C_m^\dagger C_m \rho_S + \rho_S C_m^\dagger C_m) + \sum_m C_m \rho_S C_m^\dagger . \tag{46}$$

This type of relaxation operators is very general and is found in most of the quantum optics problems involving dissipation. In (46), the C_m's are operators acting in the space of the small system. Depending on the nature of the problem there can be one, a few or an infinity of these operators.

For the particular case of spontaneous emission by a two-level system without Zeeman degeneracy, there is just a single operator $C_1 = \sqrt{\Gamma}\sigma^-$ in the relaxation operator (46):

$$\mathscr{L}_{\text{relax}}(\rho_S) = -\frac{\Gamma}{2}(\sigma^+\sigma^-\rho_S + \rho_S\sigma^+\sigma^-) + \Gamma\sigma^-\rho_S\sigma^+ \tag{47}$$

with

$$\sigma^+ = |e\rangle\langle g|\,, \qquad \sigma^- = |g\rangle\langle e|\,. \tag{48}$$

One can check that this form of $\mathscr{L}_{\text{relax}}$ indeed leads to the well-known relaxation part of the optical Bloch equations:

$$\begin{cases}(\dot\rho_S)_{ee} = -\Gamma(\rho_S)_{ee}\,,\\ (\dot\rho_S)_{gg} = \Gamma(\rho_S)_{ee}\,,\end{cases} \qquad \begin{cases}(\dot\rho_S)_{eg} = -(\Gamma/2)(\rho_S)_{eg}\,,\\ (\dot\rho_S)_{ge} = -(\Gamma/2)(\rho_S)_{ge}\,.\end{cases} \tag{49}$$

We now present the procedure for evolving wave functions of the small system. Consider at time t that the system is in a state with the normalized wave function $|\phi(t)\rangle$. In order to get the wave function at time $t + \delta t$, we proceed in two steps:

1) First we calculate the wave function $|\phi^{(1)}(t+\delta t)\rangle$ obtained by evolving $|\phi(t)\rangle$ with the non-Hermitian Hamiltonian

$$H = H_S - \frac{i\hbar}{2}\sum_m C_m^\dagger C_m\,. \tag{50}$$

This gives for sufficiently small δt

$$|\phi^{(1)}(t+\delta t)\rangle = \left(1 - \frac{iH\delta t}{\hbar}\right)|\phi(t)\rangle. \tag{51}$$

Since H is not Hermitian, this new wave function is clearly not normalized. The square of its norm is

$$\langle\phi^{(1)}(t+\delta t)\,|\,\phi^{(1)}(t+\delta t)\rangle = \langle\phi(t)|\left(1 + \frac{iH^\dagger\delta t}{\hbar}\right)\left(1 - \frac{iH\delta t}{\hbar}\right)|\,\phi(t)\rangle = 1 - \delta p\,, \tag{52}$$

where δp reads

$$\delta p = \delta t\,\frac{i}{\hbar}\,\langle\phi(t)|\,H - H^\dagger\,|\,\phi(t)\rangle = \sum_m \delta p_m\,, \tag{53}$$

$$\delta p_m = \delta t\langle\phi(t)|\,C_m^\dagger C_m\,|\,\phi(t)\rangle \geq 0\,. \tag{54}$$

The magnitude of the step δt is adjusted so that this calculation at first order is valid; in particular it requires $\delta p \ll 1$.

For the particular case of the two-level atom problem (47), the non-Hermitian Hamiltonian is

$$H = H_S - \frac{i\hbar\Gamma}{2} |e\rangle\langle e| . \tag{55}$$

This amounts to adding the imaginary term $-i\hbar\Gamma/2$ to the energy of the unstable excited state, as usual in scattering theory.

2) The second step of the evolution of $|\phi\rangle$ between t and $t + \delta t$ consists in a possible «quantum jump» (fig. 13). The various possible «directions» for those jumps are given by the C_m operators, and the probability for making a jump in the «direction» of a particular C_m is δp_m given in (54). The new normalized wave function after such a jump is given by

$$|\phi(t + \delta t)\rangle = \frac{C_m |\phi(t)\rangle}{\| C_m |\phi(t)\rangle \|} \qquad \text{with probability } \delta p_m . \tag{56}$$

Using (53), we find that the total probability for making a jump is δp. In the no-jump case, which occurs then with a probability $1 - \delta p$, we take as new normalized wave function at time $t + \delta t$:

$$|\phi(t + \delta t)\rangle = \frac{|\phi^{(1)}(t + \delta t)\rangle}{\| |\phi^{(1)}(t + \delta t)\rangle \|} \qquad \text{with probability } 1 - \delta p = 1 - \sum_m \delta p_m . \tag{57}$$

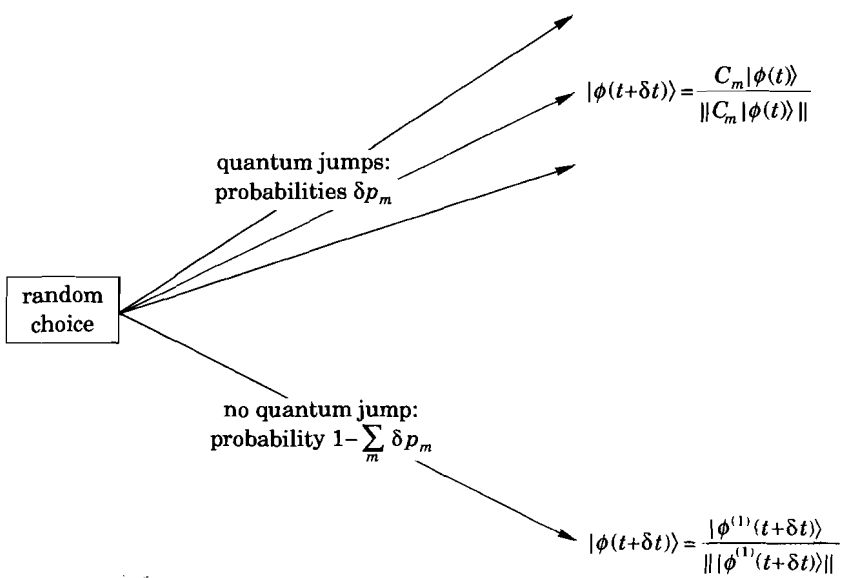

Fig. 13. – The possible quantum jumps in the Monte Carlo evolution.

Consider again as an example the particular case of the spontaneous emission of a two-level atom. The wave function at time t can be written as

$$|\phi(t)\rangle = \alpha(t)|e\rangle + \beta(t)|g\rangle. \tag{58}$$

Since there is a single C_m operator in this case, there is only one possible type of quantum jump. The probability for this quantum jump is

$$\delta p = \Gamma |\alpha|^2 \, \delta t, \tag{59}$$

and the wave function after the jump, deduced from (48) and (56), is simply $|\phi(t + \delta t)\rangle = |g\rangle$. If no jumps occur, the wave function at time $t + \delta t$ is similar to (58), with the coefficients $\alpha(t + \delta t)$ and $\beta(t + \delta t)$ deduced from $\alpha(t)$ and $\beta(t)$ using the evolution with the non-Hermitian Hamiltonian (55). Therefore, we see for this particular case that the Monte Carlo evolution can be understood as the stochastic evolution of the atomic wave function if a continuous detection of the emitted photons is performed. The probability of detecting a photon during a particular time step δt is indeed equal to δp given in (59), and the new wave function after the detection, according to the standard quantum measurement theory, corresponds to the atom in its ground state g.

It is actually quite a general result that the Monte Carlo evolution outlined above represents a possible history of the system wave function with a suitable continuous-detection process taking place [43, 45]. Consequently, although this procedure does not make any reference to measurements on the system, it is often useful, in order to get some physical understanding for the result of the simulation, to refer to such a continuous-detection process as if it was really performed.

4·2. *Equivalence with the master equation.* – With this set of rules we can propagate a wave function $|\phi(t)\rangle$ in time, and we now show that this procedure is equivalent to the master equation (45). More precisely we consider the quantity $\bar{\sigma}(t)$ obtained by averaging $\sigma(t) = |\phi(t)\rangle\langle\phi(t)|$ over the various possible outcomes at time t of the MCWF evolutions all starting in $|\phi(0)\rangle$, and we prove that $\bar{\sigma}(t)$ coincides with $\rho_S(t)$ at all times t, provided they coincide at $t = 0$.

Consider a MCWF $|\phi(t)\rangle$ at time t. At time $t + \delta t$, the average value of $\sigma(t + \delta t)$ is

$$\overline{\sigma(t + \delta t)} = (1 - \delta p) \frac{|\phi^{(1)}(t + \delta t)\rangle}{\||\phi^{(1)}(t + \delta t)\rangle\|} \frac{\langle\phi^{(1)}(t + \delta t)|}{\||\phi^{(1)}(t + \delta t)\rangle\|} + \tag{60}$$

$$+ \sum_m \delta p_m \frac{C_m|\phi(t)\rangle}{\|C_m|\phi(t)\rangle\|} \frac{\langle\phi(t)|C_m^\dagger}{\|C_m|\phi(t)\rangle\|}$$

which gives, using (51), (52) and (56),

$$\overline{\sigma(t+\delta t)} = \sigma(t) + \frac{i\,\delta t}{\hbar}[\sigma(t), H_S] + \delta t\, \mathscr{L}_{\text{relax}}(\sigma(t)). \tag{61}$$

We now average this equation over the possible values of $\sigma(t)$ and we obtain

$$\frac{d\bar{\sigma}}{dt} = \frac{i}{\hbar}[\bar{\sigma}, H_S] + \mathscr{L}_{\text{relax}}(\bar{\sigma}). \tag{62}$$

This equation is identical to the master equation (45). If we assume that $\rho_S(0) = |\phi(0)\rangle\langle\phi(0)|$, $\bar{\sigma}(t)$ and $\rho_S(t)$ coincide at any time, which demonstrates the equivalence between the two points of view. In the case where $\rho_S(0)$ does not correspond to a pure state, one has first to decompose it as a statistical mixture of pure states, $\rho(0) = \sum p_i |\chi_i\rangle\langle\chi_i|$, and then randomly choose the initial MCWFs among the $|\chi_i\rangle$ with the probability law p_i.

As mentioned in the introduction, the master-equation approach and the reduced density matrix give access to one-time average values $a(t) = \langle A\rangle(t) = \mathrm{Tr}(\rho_S(t)A)$, which can now also be obtained with the MCWF method. One calculates, for several outcomes $|\phi^{(i)}(t)\rangle$ of the MCWF evolution, the quantum average $\langle\phi^{(i)}(t)|A|\phi^{(i)}(t)\rangle$, and one takes the mean value of this quantity over the various outcomes $|\phi^{(i)}(t)\rangle$:

$$\langle A\rangle_{(n)}(t) = \frac{1}{n}\sum_{i=1}^{n}\langle\phi^{(i)}(t)|A|\phi^{(i)}(t)\rangle. \tag{63}$$

For n sufficiently large, (62) implies that $\langle A\rangle_{(n)}(t) \simeq \langle A\rangle(t)$.

As an example of the agreement between the master-equation approach and the MCWF approach, we have calculated by those two methods the excited-state population of a two-level atom coupled to a coherent laser field. The parameters for this Rabi nutation are a zero detuning δ between the laser and atomic frequencies, and a Rabi frequency $\Omega = 3\Gamma$. In fig. 14*a*), we show this excited-state population for a single «history» for $|\phi(t)\rangle$. One finds, as expected, a continuous evolution for this population oscillating between 0 and 1, with random quantum jumps projecting the atomic wave function into the ground state. In fig. 14*b*), we indicate the MCWF result obtained with the average of 100 wave functions. It shows a damped oscillation as a result of the dephasing of the individual oscillations due to the randomness of the various quantum jumps. This MCWF result is in very good agreement with the one derived from the master equation (optical Bloch equations).

As appears clearly in the proof, the equivalence of the master-equation and MCWF approaches does not depend on the particular value of the time step δt. From a practical point of view, the largest possible δt is preferable, and one might benefit from using a generalization of (51) to a higher order in δt, as, for example, a 4th-order Runge-Kutta-type calculation. The only requirement on δt

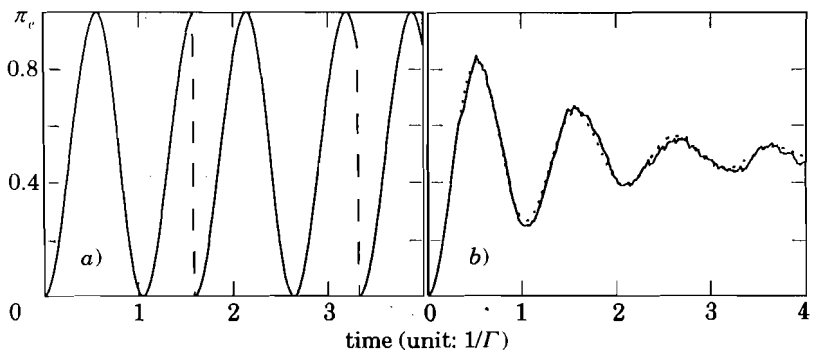

Fig. 14. – *a*) Time evolution of the excited-state population of a two-level atom in the MCWF approach. The dashed lines indicate the projection of the atomic wave function onto the ground state (quantum jump). *b*) Excited-state population averaged over 100 MCWF starting all in ground state at time 0. The dotted line represents the master-equation result.

is that the various $\eta_i \delta t$, where the $\hbar\eta_i$ are the eigenvalues of H, should be small compared to 1. Of course, we assume here that those eigenvalues have been simplified as much as possible in order to eliminate the bare energies of the eigenstates of H_S. For instance, for a two-level atom with a transition frequency ω_A coupled to a laser field with frequency ω_L, one makes the rotating-wave approximation in the rotating frame so that the $|\eta_i|$'s are of the order of the natural width Γ, the Rabi frequency Ω or the detuning $\delta = \omega_L - \omega_A$; they are consequently much smaller than ω_A.

One might wonder whether there is a minimal size for the time step δt. In the derivation presented above, it can be chosen arbitrarily small. However, one should remember that the derivation of (45) involves a coarse-grain average of the real density operator evolution. The time step of this coarse-grain average has to be much larger than the correlation time τ_c of the reservoir, which is typically an optical period for the problem of spontaneous emission. Therefore, one should be cautious when considering any result derived from this MCWF approach involving details with a time scale of the order of or shorter than τ_c, and only δt larger than τ_c should be applied. This appears clearly if one starts directly from the interaction Hamiltonian between the system and the reservoir in order to generate the stochastic evolution for the system wave function [43]. The condition $\delta t \gg \tau_c$ is then required to prevent quantum Zeno-type effects [47]. This restriction is discussed in detail in [48] in connection with quantum measurement theory.

4·3. *Connection with previous works.* – The problem of stochastic wave function evolution in connection with the treatment of dissipative systems in quantum optics has recently received a lot of attention. In the context of nonclassical

field generation, CARMICHAEL [45] has proposed an approach named «quantum trajectories», inspired by the theory of photoelectron counting sequences [49] and quite similar to the spirit of the present work.

For simple atomic systems (2 or 3 levels) coupled to the electromagnetic field, the dynamics can be interpreted in terms of one or a few *delay functions*, which give the probability distribution of the time intervals between the emission of two successive photons [50-52]. When this function is known analytically, it can generate a very efficient Monte Carlo analysis of the process: just after the emission of the n-th fluorescence photon at time t_n, the atom is in its ground state and the choice of a single random number is sufficient to determine the time t_{n+1} of emission of the $(n + 1)$-th photon. This type of Monte Carlo analysis has been used in [53] to simulate an atomic-beam cooling experiment, and in [51] to prove numerically the existence of dark periods in the fluorescence of a 3-level atom (quantum jumps). Very recently, laser cooling of atoms using velocity-selective coherent population trapping [54] and lasing without inversion [55] have been analysed by this type of Monte Carlo method.

Unfortunately, the delay function cannot be calculated analytically for complex systems involving a large number of levels. Nevertheless, it is possible to generate a Monte Carlo solution for this problem in which a single random number determines the time of emission of each fluorescence photon [46]. The evolution of the system between two quantum jumps has to be integrated step by step numerically, so that the amount of calculation involved is similar to the one required by the method presented in this lecture.

Another class of stochastic equations for system wave functions, which is also equivalent to the master equation (45), has been introduced by GISIN and PERCIVAL [56] (see also the work by DIÓSI [57]). In this approach, only continuous stochastic equations are considered. CARMICHAEL has shown that, for the particular case of the homodyne detection of the fluorescence light, the quantum jump formalism can be transformed into such a continuous stochastic equation [45]. Actually this proof can be extended to the most general case [58].

4·4. *Application to laser cooling.* – We now focus on the case of 1D Doppler cooling of a two-level atom, for which we present some numerical results. This will give an illustration of the effectiveness of the MCWF method as compared with the master-equation approach for studying laser cooling in the quantum regime.

4·4.1. The model. We consider here Doppler cooling of a two-level atom, as has already been described in subsect. 2·3: Doppler cooling originates from the fact that an atom moving in the field of a standing wave is closer to resonance with the counterpropagating component of the wave than with the copropagating one; the atom, therefore, feels a net radiation pressure force opposed to its velocity. This picture works well at nonsaturating laser intensities,

where one can add the effect of the two waves independently. At higher intensities this semi-classical analysis becomes more complicated [59, 60] and a quantum treatment of the atomic external motion is a good alternative. We present here the result of such a treatment using both a master-equation and a MCWF approach.

The Hamiltonian H_S reads here, using the rotating-wave approximation,

$$H_S = \frac{P^2}{2M} + \hbar\Omega\cos(kZ)(\sigma^+ + \sigma^-) - \hbar\delta P_e\,, \tag{64}$$

where Z and P are the atomic position and momentum operators and Ω is the Rabi frequency of each travelling wave forming the standing wave. We choose the initial wave function $|\phi(0)\rangle$ equal to $|g, p = 0\rangle$. At a time t, $|\phi(t)\rangle$ can be written

$$|\phi(t)\rangle = \sum_n \alpha_n(t)|g, p = p_0 + 2n\hbar k\rangle + \beta_n(t)|e, p = p_0 + (2n+1)\hbar k\rangle, \tag{65}$$

where the momentum p_0 depends on the random recoils which have occurred between 0 and t, and remains constant between two quantum jumps. According to subsect. 2·2, the evolution of α_n and β_n consists of sequences of two steps. First the wave function evolves linearly with the non-Hermitian Hamiltonian $H = H_S - i\hbar\Gamma|e\rangle\langle e|/2$:

$$i\dot{\alpha}_n = \frac{(p_0 + 2n\hbar k)^2}{2M\hbar}\alpha_n + \frac{\Omega}{2}(\beta_n + \beta_{n-1}), \tag{66}$$

$$i\dot{\beta}_n = \left(\frac{(p_0 + (2n+1)\hbar k)^2}{2M\hbar} - \delta - \frac{i\Gamma}{2}\right)\beta_n + \frac{\Omega}{2}(\alpha_n + \alpha_{n+1}). \tag{67}$$

Then we randomly decide whether a quantum jump occurs. The probability δp for a jump is proportional to the total excited-state population:

$$\delta p = \Gamma\sum_n |\beta_n|^2\,\delta t\,. \tag{68}$$

If no quantum jump occurs, we simply normalize the wave function. If a quantum jump occurs, the momentum $\hbar k'$ along the z-axis of the fluorescence photon is chosen randomly with a probability law deduced from the dipole radiation pattern, which leads to [44]

$$\alpha_n(t + \delta t) = \mu\beta_n(t)\,, \tag{69}$$

$$\beta_n(t + \delta t) = 0\,, \tag{70}$$

$$p_0 \to p_0 - \hbar k'\,, \tag{71}$$

where μ is a normalization coefficient. We note that in this way the recoil due to spontaneous emission is treated in an exact manner. In the master-equation approach, an exact treatment of the spontaneous recoil requires a discretization of

atomic momenta on a grid with a step size smaller than $\hbar k$. This increases the amount of calculation of the master equation with respect to the MCWF one, in addition to the N *vs.* N^2 argument mentioned in the introduction (*).

In order to make a fair comparison between the two approaches, we have chosen a coarse discretization for the atomic momentum, with a step size $\hbar k$, *i.e.* $k' = -k$, 0 or k and a probability law $1/5:3/5:1/5$, which gives an optimum representation of the diffusion rate due to the directional distribution of spontaneously emitted photons.

4·4.2. Numerical results. We have considered the case of sodium atoms for which the Doppler-cooling limit (22) corresponds to $p_{\text{r.m.s.}} \simeq 8.4\,\hbar k$. We have discretized the momentum between $-50\,\hbar k$ and $+50\,\hbar k$ which corresponds to a basis with 202 eigenstates in total, with at any time 101 nonzero coefficients α_n and β_n (see (65), where p_0 is either an odd or even multiple of $\hbar k$).

The results for the evolution of the sample mean $\langle P^2 \rangle_{(n)}$, defined as

$$\langle P^2 \rangle_{(n)}(t) = \frac{1}{n} \sum_{i=1}^{n} \langle \phi^{(i)}(t) | P^2 | \phi^{(i)}(t) \rangle , \tag{72}$$

are given in fig. 15 together with the results for $\langle P^2 \rangle(t)$ obtained using the master-equation treatment. These results correspond to the parameters $\Omega = -\delta = \Gamma/2$. The MCWF results have been obtained with the average of $n = 500$ evolutions.

We have indicated in fig. 15 the statistical error $\delta P^2_{(n)}$ on the determination of $\langle P^2 \rangle_{(n)}$ (see [44] for details). This quantity $\delta P^2_{(n)}$ gives an estimate of the quality of the result, and, with $n = 500$ wave functions, the *signal-to-noise* ratio in the range of 20 is quite satisfactory.

With a scalar machine, we have found that the time required for the calculation with 500 wave functions is equal to the time required for the master-equation evolution. With a vectorial compiler, we have found that there is an additional gain of a factor 15 in the benefit of the MCWF procedure. Therefore, even for this relatively simple 1D problem with «only» 200 levels, the MCWF method is at least as efficient as the master-equation approach for determining cooling limits with a good precision.

We clearly see in fig. 15 the existence of two regimes in the evolution of $\langle P^2 \rangle(t)$. At short time ($t < 200\,\Gamma^{-1}$, see insert of fig. 15), the number of spontaneous emissions is small, and the physics involved is essentially the diffraction of the plane atomic de Broglie wave by the grating formed by the laser standing wave [61]. For longer interaction times, dissipation comes into play [62, 63] and $\langle P^2 \rangle(t)$ tends to a steady-state value, of the order of $(11\,\hbar k)^2$. This value for

(*) This is the reason why fig. 8 has been obtained with a simplified dipole radiation diagram.

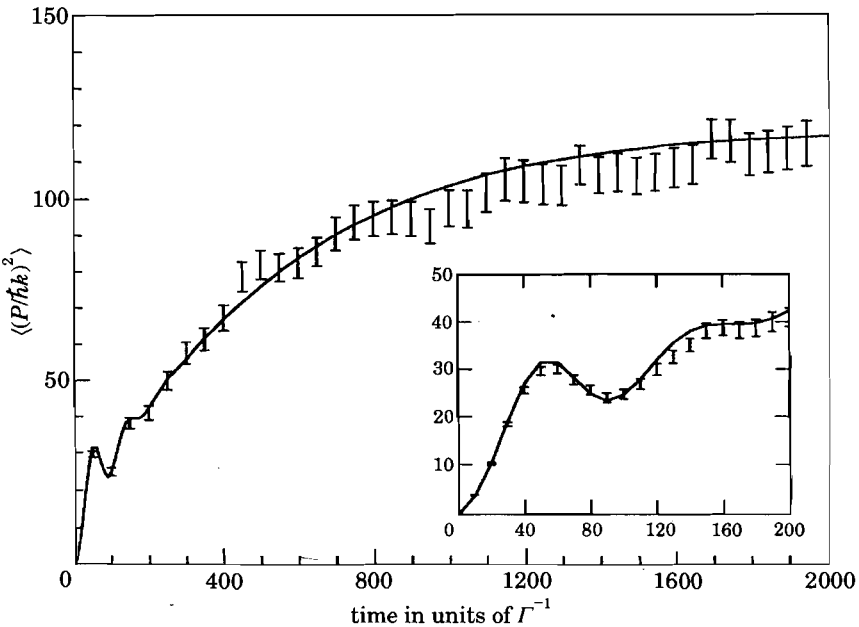

Fig. 15. – Time evolution of $\langle P^2 \rangle$ in Doppler cooling of Na atoms, with $\Omega = -\delta = \Gamma/2$. The points represent the Monte Carlo results, obtained by averaging $n = 500$ MCWF evolutions. The solid curve is the result of the density matrix approach. The insert details the short-time regime corresponding to the diffraction of the atomic de Broglie wave by the laser standing wave.

$p_{\text{r.m.s.}}$ is larger than the Doppler-cooling limit ($8.4\hbar k$) because of saturation effects.

4·5. *Conclusion for the* MCWF *approach.* – We have presented a stochastic evolution for the wave function of a system coupled to a reservoir in the Markovian regime. Each time step in this stochastic evolution consists of two parts: a non-Hermitian evolution and a possible quantum jump. We have proved the equivalence of this Monte Carlo wave function approach with the master-equation treatment.

This approach provides a computational tool which is often more efficient than the standard master-equation treatment for systems with a number of states $N \gg 1$ (for a detailed discussion see [44]). Indeed a wave function involves only N components while a density matrix is described by N^2 terms. It is, therefore, particularly well adapted to the study of laser cooling in the quantum regime. We have presented here the 1D example of Doppler cooling. This method has also been applied successfully to determine the cooling limits of the Sisyphus mechanism in 2 dimensions [35], and also to calculate the spectrum of the light emitted by an assembly of cold atoms [64]. Problems such as the study

of collisions between cold atoms, or nonlinear mixing of quantum fields may also benefit from such an approach.

We have emphasized that this simulation is in many practical cases directly connected to a measurement sequence performed on the system. Each Monte Carlo trajectory is a possible history for the individual quantum system. In this respect, the noise appearing when one simulates with this method the measurement of a given observable A is also interesting. The fluctuations in the number of occurrences of a given eigenvalue a_i of A correspond to the quantum noise that one would get in a real experiment, performing the relevant detection scheme on an individual quantum system. Since more and more quantum optics and atomic-physics experiments are now performed with a single system (single ion or atom, single mode of a cavity), Monte Carlo wave function methods should, therefore, have many applications, since they lead to predictions closer to actual experimental signals than the master equation, which rather deals with ensemble averages.

* * *

The authors are very grateful to C. COHEN-TANNOUDJI and K. MØLMER for their participation to various parts of this lecture.

REFERENCES

[1] S. CHU, L. HOLLBERG, J. BJORKHOLM, A. CABLE and A. ASHKIN: *Phys. Rev. Lett.*, **55**, 48 (1985).
[2] P. LETT, R. WATTS, C. WESTBROOK, W. PHILLIPS, P. GOULD and H. METCALF: *Phys. Rev. Lett.*, **61**, 169 (1988).
[3] C. SALOMON, J. DALIBARD, W. D. PHILLIPS, A. CLAIRON and S. GUELLATI: *Europhys. Lett.*, **12**, 683 (1990).
[4] A. ASPECT, E. ARIMONDO, R. KAISER, N. VANSTEENKISTE and C. COHEN-TANNOUDJI: *Phys. Rev. Lett.*, **61**, 826 (1988).
[5] M. KASEVICH and S. CHU: *Phys. Rev. Lett.*, **69**, 1741 (1992).
[6] M. KASEVICH, E. RIIS, S. CHU and R. DE VOE: *Phys. Rev. Lett.*, **63**, 612 (1989).
[7] A. CLAIRON, C. SALOMON, S. GUELLATI and W. D. PHILLIPS: *Europhys. Lett.*, **16**, 165 (1991).
[8] P. L. GOULD, P. D. LETT, P. S. JULIENNE, W. D. PHILLIPS, H. R. THORSHEIM and J. WEINER: *Phys. Rev. Lett.*, **60**, 788 (1988).
[9] M. PRENTISS, A. CABLE, J. E. BJORKHOLM, S. CHU, E. RAAB and D. PRITCHARD: *Opt. Lett.*, **13**, 452 (1988).
[10] A. GALLAGHER and D. E. PRITCHARD: *Phys. Rev. Lett.*, **63**, 957 (1989).
[11] P. D. LETT, P. S. JESSEN, W. D. PHILLIPS, S. L. ROLSTON, C. I. WESTBROOK and P. L. GOULD: *Phys. Rev. Lett.*, **67**, 2139 (1991).
[12] D. GRISON, B. LOUNIS, C. SALOMON, J.-Y. COURTOIS and G. GRYNBERG: *Europhys. Lett.*, **15**, 149 (1991).
[13] J. TABOSA, G. CHEN, Z. HU, R. LEE and H. J. KIMBLE: *Phys. Rev. Lett.*, **66**, 3245 (1991).

[14] See, *e.g.*, the special issue of *Applied Physics B* of May 1992 on *Optics and Interferometry with Atoms*, edited by J. MLYNECK, V. BALYKIN and P. MEYSTRE.
[15] Y. CASTIN: PhD Thesis, Université Paris 6 (February 1992).
[16] R. J. COOK: *Phys. Rev. A*, **20**, 224 (1979).
[17] J. P. GORDON and A. ASHKIN: *Phys. Rev. A*, **21**, 1606 (1980).
[18] C. COHEN-TANNOUDJI: in *Fundamental Systems in Quantum Optics, Les Houches Summer School 1990*, edited by J. DALIBARD, J.-M. RAIMOND and J. ZINN-JUSTIN (North-Holland, Amsterdam, 1992), p. 1.
[19] J. DALIBARD and C. COHEN-TANNOUDJI: *J. Phys. B*, **18**, 1661 (1985).
[20] S. STENHOLM: *Rev. Mod. Phys.*, **58**, 699 (1986).
[21] T. HÄNSCH and A. SCHAWLOW: *Opt. Commun.*, **13**, 68 (1975).
[22] D. WINELAND and H. DEHMELT: *Bull. Am. Phys. Soc.*, **20**, 637 (1975).
[23] V. G. MINOGIN and O. T. SERIMAA: *Opt. Commun.*, **30**, 373 (1979).
[24] D. J. WINELAND and W. M. ITANO: *Phys. Rev. A*, **20**, 1521 (1979).
[25] S. CHU, D. WEISS, Y. SHEVY and P. UNGAR: in *Atomic Physics 11*, edited by S. HAROCHE, J. C. GAY and G. GRYNBERG (World Scientific, Singapore, 1989), p. 636.
[26] J. DALIBARD, C. SALOMON, A. ASPECT, E. ARIMONDO, R. KAISER, N. VANSTEENKISTE and C. COHEN-TANNOUDJI: in *Atomic Physics 11*, edited by S. HAROCHE, J. C. GAY and G. GRYNBERG (World Scientific, Singapore, 1989), p. 199.
[27] P. J. UNGAR, D. S. WEISS, E. RIIS and S. CHU: *J. Opt. Soc. Am. B*, **6**, 2058 (1989).
[28] J. DALIBARD and C. COHEN-TANNOUDJI: *J. Opt. Soc. Am. B*, **6**, 2023 (1989).
[29] More complex polarization configurations leading to mixed types of cooling can also be considered: V. FINKELSTEIN, P. R. BERMAN and J. GUO: *Phys. Rev. A*, **45**, 1829 (1992).
[30] Y. CASTIN, J. DALIBARD and C. COHEN-TANNOUDJI: *Proceedings of the LIKE Workshop 1990*, in *Light Induced Kinetic Effects on Atoms, Ions and Molecules*, edited by L. MOI, S. GOZZINI, C. GABBANINI, E. ARIMONDO and F. STRUMIA (ETS Editrice, Pisa, 1991), p. 5.
[31] Y. CASTIN and J. DALIBARD: *Europhys. Lett.*, **14**, 761 (1991).
[32] P. VERKERK, B. LOUNIS, C. SALOMON, C. COHEN-TANNOUDJI, J.-Y. COURTOIS and G. GRYNBERG: *Phys. Rev. Lett.*, **68**, 3861 (1992).
[33] P. S. JESSEN, C. GERZ, P. D. LETT, W. D. PHILLIPS, S. L. POLSTON, R. J. C. SPREEUW and C. I. WESTBROOK: *Phys. Rev. Lett.*, **69**, 49 (1992).
[34] R. GUPTA, S. PADUA, T. BERGEMAN and H. METCALF: in *Proc. S.I.F., Course CXVIII*, edited by E. ARIMONDO, W. D. PHILLIPS and F. STRUMIA (North-Holland, Amsterdam, 1992), p. 345; R. GUPTA, S. PADUA, C. XIE, H. BATELAAN, T. BERGEMAN and H. METCALF: poster at ICAP XIII (August 1992).
[35] C. BERG-SØRENSEN, K. MØLMER, Y. CASTIN and J. DALIBARD: poster at ICAP XIII (August 1992).
[36] T. BERGEMAN: poster at ICAP XIII (August 1992).
[37] J.-Y. COURTOIS and G. GRYNBERG: *Phys. Rev. A*, **46**, 7060 (1992).
[38] W. H. LOUISELL: *Quantum Statistical Properties of Radiation* (Wiley, New York, N.Y., 1973).
[39] F. HAAKE: *Statistical Treatment of Open Systems by Generalized Master Equations, Springer Tracts in Modern Physics*, Vol. **66**, edited by G. HOHLER (Springer, Berlin, 1973), p. 98.
[40] C. COHEN-TANNOUDJI: in *Les Houches 1975, Frontiers in Laser Spectroscopy*, edited by R. BALIAN, S. HAROCHE and S. LIBERMAN (North Holland, Amsterdam, 1977), p. 3.
[41] C. W. GARDINER: *Handbook of Stochastic Methods* (Springer, Berlin, 1983).

[42] M. LAX: *Phys. Rev.*, **172**, 350 (1968).
[43] J. DALIBARD, Y. CASTIN and K. MØLMER: *Phys. Rev. Lett.*, **68**, 580 (1992).
[44] K. MØLMER, Y. CASTIN and J. DALIBARD: *J. Opt. Soc. Am. B*, **10**, 524 (1993).
[45] H. J. CARMICHAEL: lecture notes at U.L.B., Fall 1991 (unpublished); see also H. J. CARMICHAEL and L. TIAN: in *OSA Annual Meeting Technical Digest* 1990, p. 3.
[46] R. DUM, P. ZOLLER and H. RITSCH: *Phys. Rev. A*, **45**, 4879 (1992); R. DUM, A. S. PARKINS, P. ZOLLER and C. W. GARDINER: *Phys. Rev. A*, **46**, 4382 (1992).
[47] B. MISRA and E. C. G. SUDARSHAN: *J. Mat. Phys. (N.Y.)*, **18**, 756 (1977).
[48] G. C. HEGERFELDT and T. S. WILSER: in *II International Wigner Symposium, July 1991, Goslar*, proceedings to be published by World Scientific.
[49] P. L. KELLEY and W. H. KLEINER: *Phys. Rev.*, **136**, A316 (1964).
[50] C. COHEN-TANNOUDJI and J. DALIBARD: *Europhys. Lett.*, **1**, 441 (1986).
[51] P. ZOLLER, M. MARTE and D. F. WALLS: *Phys. Rev. A*, **35**, 198 (1987).
[52] H. J. CARMICHAEL, S. SINGH, R. VYAS and P. R. RICE: *Phys. Rev. A*, **39**, 1200 (1989).
[53] R. BLATT, W. ERTMER, P. ZOLLER and J. L. HALL: *Phys. Rev. A*, **34**, 3022 (1986).
[54] C. COHEN-TANNOUDJI, F. BARDOU and A. ASPECT: in *Laser Spectroscopy X, 1991*, edited by M. DUCLOY, E. GIACOBINO and G. CAMY (World Scientific, Singapore, 1992), p. 3.
[55] C. COHEN-TANNOUDJI, B. ZAMBON and E. ARIMONDO: *C. R. Acad. Sci.*, **314**, 1139, 1293 (1992).
[56] N. GISIN: *Phys. Rev. Lett.*, **52**, 1657 (1984); *Helv. Phys. Acta*, **62**, 363 (1989); N. GISIN and I. PERCIVAL: *Phys. Lett. A*, **167**, 315 (1992).
[57] L. DIÓSI: *J. Phys. A*, **21**, 2885 (1988).
[58] Y. CASTIN, J. DALIBARD and K. MØLMER: *Proceedings of the I.C.A.P. XIII*, edited by T. W. HÄNSCH and H. WALTHER (August 1992).
[59] V. G. MINOGIN: *Sov. Phys. JETP*, **53**, 1164 (1981).
[60] K. BERG-SØRENSEN, E. BONDERUP, K. MØLMER and Y. CASTIN: *J. Phys. B*, **25**, 4195 (1992).
[61] C. TANGUY, S. REYNAUD and C. COHEN-TANNOUDJI: *J. Phys. B*, **17**, 4623 (1984).
[62] M. WILKENS, E. SCHUMACHER and P. MEYSTRE: *Opt. Commun.*, **86**, 34 (1991).
[63] S. STENHOLM: in *Proc. S.I.F., Course CXVIII*, edited by E. ARIMONDO, W. D. PHILLIPS and F. STRUMIA (North-Holland, Amsterdam, 1992), p. 29.
[64] P. MARTE, R. DUM, R. TAIEB, P. LETT and P. ZOLLER: *Phys. Rev. Lett.*, **71**, 1335 (1993).